



The EarthCARE Mission: Science Data Processing Chain Overview

Michael Eisinger¹, Fabien Marnas², Kotska Wallace², Takuji Kubota³, Nobuhiro Tomiyama³,
Yuichi Ohno⁴, Toshiyuki Tanaka³, Eichi Tomita³, Tobias Wehr^{2,†}, and Dirk Bernaerts²

¹European Space Agency, ESA-ECSAT, Fermi Avenue, Didcot OX11 0FD, United Kingdom

²European Space Agency, ESA-ESTEC, Keplerlaan 1, 2201 AZ Noordwijk, The Netherlands

³Japan Aerospace Exploration Agency (JAXA), 305-8505 2 Chome-1-1, Sengen, Tsukuba, Ibaraki, Japan

⁴National Institute of Information and Communications Technology (NICT), 184-0015 4 Chome-2-1, Nukui Kitamachi, Koganei, Tokyo, Japan

[†]deceased, 1 February 2023

Correspondence: Michael Eisinger (Michael.Eisinger@esa.int)

Abstract. The Earth Cloud Aerosol and Radiation Explorer (EarthCARE) is a satellite mission implemented by the European Space Agency (ESA) in cooperation with the Japan Aerospace Exploration Agency (JAXA) to measure global profiles of aerosols, clouds and precipitation properties together with radiative fluxes and derived heating rates. The data will be used in particular to evaluate the representation of clouds, aerosols, precipitation and associated radiative fluxes in weather forecasting and climate models.

The science data acquired by the four satellite instruments are processed on ground. Calibrated instrument data – level 1 data products – and retrieved geophysical data products – level 2 data products – are produced in the ESA and JAXA ground segments. This paper provides an overview of the data processing chains of ESA and JAXA and explains the instrument level 1 data products and main aspects of the calibration algorithms. Furthermore, an overview of the level 2 data products, with references to the respective dedicated papers, is provided.

1 Introduction

The Intergovernmental Panel on Climate Change (IPCC, 2023) has recognised that:

While major advances in the understanding of cloud processes have increased the level of confidence and decreased the uncertainty range for the cloud feedback by about 50 % compared to AR5, clouds remain the largest contribution to overall uncertainty in climate feedbacks (high confidence).

The Earth Cloud, Aerosol and Radiation Explorer (EarthCARE) mission will allow scientists to address this uncertainty, enabling a direct verification of the impact of clouds and aerosols on atmospheric heating rates and radiative fluxes. The collection of global cloud, aerosol and precipitation profiles, along with co-located radiative flux measurements, will be used to evaluate their representation in weather forecast and climate models, with the objective to improve parameterisation schemes. EarthCARE is an ESA Explorer mission that is being carried out in a collaboration with JAXA, which is providing one of the instruments. A mission overview by Wehr et al. (2023) describes the mission, its science objectives, observational require-



ments, ground and space segments. EarthCARE will fly in a sun-synchronous, low-Earth orbit, with a Mean Local Solar Time of 14:00 \pm 5 minutes and a 25-day repeat cycle. It will fly at a rather low altitude in order to maximise performance of the active instruments with respect their power needs. The satellite embarks four instruments: the ATmospheric LIDar (ATLID),
25 the Cloud Profiling Radar (CPR), the Multi-Spectral Imager (MSI) and the Broad-Band Radiometer (BBR). The UV lidar, equipped with a high-spectral-resolution receiver and depolarisation measurement channel, will measure vertical profiles of aerosols and thin clouds and allow for classification of five aerosol types. The highly sensitive 94 GHz (W-band) cloud radar will provide measurements of clouds and precipitation. Its sensitivity partly overlaps with the lidar but its signal can penetrate through, or deep into, the cloud, beyond where the lidar signal attenuates. Furthermore, it has Doppler capability, allowing
30 measurement of the vertical velocity of cloud particles. The imager has four solar and three thermal channels that will provide across-track swath information on clouds and aerosols, and facilitate construction of 3D cloud-aerosol-precipitation scenes for radiative transfer calculations. The Broad-Band Radiometer measures solar and thermal radiances in three fixed viewing directions, along the flight track, which will be used to derive the top-of-atmosphere flux estimates. ATLID and CPR data will be used to calculate atmospheric heating rates and radiative fluxes, using 1D and 3D radiative transfer models, which results
35 can be compared against the flux estimated from EarthCARE Broad-Band Radiometer measurements.

Science data acquired by the instruments will be processed in ground segments at both Europe and Japan. As well as the four level 1 instrument data streams, a particular aspect of the EarthCARE mission is the large number of level 2 data products that will be generated in order to retrieve a variety of geophysical data products (see section 8.2 in Wehr et al. (2023) for a description of product levels). These will take advantage of the synchronous data from multiple instrument sources, as well
40 as making use of a dedicated, auxiliary stream of meteorological data that will be provided from the European Centre for Medium Range Weather Forecasting (ECMWF). The purposes of the data products cover, for example, target classification, vertical profiles of microphysical properties of ice, mixed and liquid clouds, particle fall speed, precipitation parameters, and aerosol type. This paper gives an overview of the processing chain development, the scientific data products and their retrieval algorithms, simulation and testing. Section 2 provides an overview of the processing chains at ESA and JAXA, illustrating
45 the production model. Section 3 is dedicated to the level 1 data processors and products for the four EarthCARE instruments. Section 4 describes the auxiliary data processors and products, which make use of meteorological data from ECMWF and provide a common spatial grid for synergistic processors. Section 5 describes the level 2 processors and products, developed in Europe, Japan and Canada. Section 6 gives an overview of the development that has been undertaken for the processing chain, end-to-end simulator (E3SIM), generation and use of test data sets, and some of the lessons that have been learnt. Section 7
50 provides useful information concerning product format and conventions.

2 Processing chains

Instrument data is transmitted in Instrument Source Packets (ISP), from the satellite to ground, via the satellite's X-band antenna and enters the Payload Data Ground Segment (PDGS). As one of its responsibilities the PDGS processes the ISP data to release a range of data products. It also monitors the data quality and performs the mission planning, including for



55 instrument calibration activities. PDGS initial processing takes ISPs and marshals them into a consecutive time sequence in an individual level 0 product for each instrument, annotated with ancillary data that is also contained in the ISPs. The instrument level 1 processors take as their input these level 0 products and create level 1b products that are fully calibrated and geolocated instrument science measurements on the native instrument grid for ATLID, MSI and the BBR single pixel product. The nominal BBR product is integrated 10 km along track. Additionally an MSI level 1c product is produced, with interpolation to a spatial grid common to all MSI bands. CPR level 1 data is produced by JAXA and made available at the PDGS for use in the level 2 processors.

Additionally there are two auxiliary products that are introduced into the processing chain. These are ECMWF meteorological fields limited to EarthCARE swath and a spatial grid shared by all instruments (“joint standard grid”).

65 The PDGS performs an instrument data calibration and monitoring function at the Instrument Calibration and Monitoring Facility (ICMF). Data, generally at L1, from routine on-orbit calibrations of the three European instruments is plotted and reviewed at pre-specified intervals, in order to assess whether it is necessary to, for instance, modify a parameter (set) in the Calibration and Characterisation Database (CCDB) or perform an additional calibration. During the mission’s operating phase, data quality will also be monitored by a team, with members from ESA and the science user community, that assesses the geophysical data products.

70 **2.1 ESA processing chain**

The complete set of ESA data products, plus JAXA’s CPR level 1b product, is generated according to the ESA EarthCARE Production Model, depicted in Fig. 1. It includes level 0, level 1 and level 2 data products, as well as auxiliary and supporting data products. The processing chain is run at the PDGS, with two exceptions: the CPR level 1b product (section 3.2) is generated in the JAXA ground segment using a data processor developed by JAXA, and the X-MET data product (section 4.1) is produced at ECMWF using a data processor developed by ESA.

Level 2 products are distinguished between level 2a (L2a) and level 2b (L2b). L2a refers to a data product derived from only one EarthCARE instrument, for example, ATLID. L2b refers to a data product derived from two or more instruments, for example, AC-TC is the target classification (TC) synergistically derived from ATLID (A) and CPR (C).

Every data product is produced by a processor. A processor either produces one data product or more than one data product. 80 If a processor produces only one data product, the name of the processor and the name of the data product is the same. For example, the C-CLD processor produces only the C-CLD data product and the A-FM processor produces only the A-FM data product. If a processor produces more than one data product then it has a name different from the products. For example, the A-PRO processor produces the data products A-AER, A-ICE, A-TC and A-EBD. Fig. 1 gives an overview of all ESA processors and data products, including their inter-dependencies. If several data products are produced by one processor, this is indicated by a solid line around the respective data products, with the name of the processor given, for example, C-PRO and A-PRO. If a processor produces only one data product, the processor name is not explicitly indicated, as it is the same as the data product’s name. For the data product user, the name of the processor is, however, not relevant. All data products can be fully identified by their data product name only.

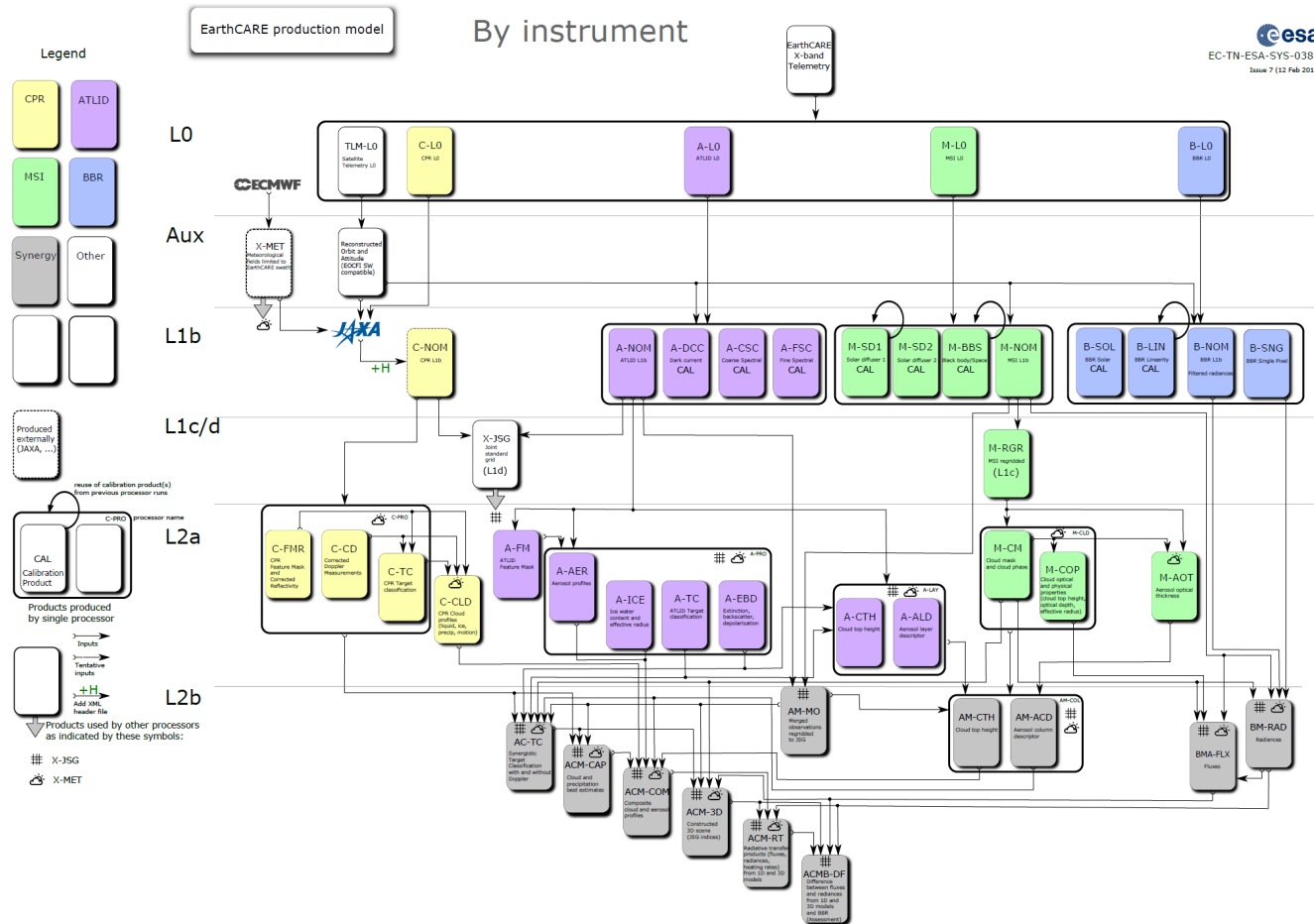


Figure 1. The ESA "EarthCARE Production Model" shows all ESA data products and the CPR level 1b product (C-NOM), which is produced by JAXA. Level 1 products (L1b, L1c/d) and auxiliary data (Aux) products are described in sections 3 and 4 respectively. Level 2 products and their retrieval algorithms (L2a, L2b) are described in this AMT Special Issue according to Table 1 (L2a) and Table 3 (L2b).

2.2 JAXA processing chain

90 The Production Model for JAXA products is illustrated in Fig. 2, showing the flow of the processors/algorithms from L1 to L2 products. Level 2 (L2) is categorized into L2a and L2b with the same definition as ESA products; L2a products are those retrieved from a single instrument, while L2b products are those derived from multiple instruments.

JAXA data products are categorized into two groups: Standard Products and Research Products. All products fall into one of the two categories, depending on the maturity of their algorithm development. Standard products (Research products) are indicated in solid-line (dashed-line) boxes in Fig. 2, respectively. The differences in the Standard Product and the Research Products are;

95



– Standard Product

1. The algorithms in the Standard Products are relatively mature and have heritage from past studies.
2. Standard products are strongly promoted to be developed and released.
- 100 3. Products are processed in the JAXA Mission Operation System and released from JAXA G-Portal website (<https://www.gportal.jaxa.jp>), together with the standard products of other JAXA Earth observation satellite missions.

– Research Product

1. The algorithms in the Research Products consist of new research developments that are challenging, yet scientifically valuable.
- 105 2. Research products are promoted to be developed and released.
3. Products will be processed and released from JAXA Earth Observation Research Center (<https://www.eorc.jaxa.jp/EARTHCARE/index.html>) and/or Japanese institute/universities.

3 Level 1 data processors and products

3.1 ATLID

110 The High Spectral Resolution Lidar, ATLID, will measure vertically resolved profiles (pure atmospheric and ground-backscattered optical power) over 3 optical paths. In order to increase the signal to noise ratio, it is possible to integrate two consecutive lidar shots.

- 115 1. Mie co-polar channel: which is the backscattered signal, co-polarised with respect to laser transmission, received within the transmission bandwidth of the High Spectral Resolution Etalon (HSRE). It represents mostly the particles signature, with narrow spectral broadening.
2. Rayleigh (co-polar) channel: which is the backscattered signal, co-polarised with respect to laser transmission, reflected by the HSRE. It represents mostly the molecules signature, with Rayleigh broadening.
3. Cross-polar channel: which is the total backscattered signal (Mie + Rayleigh), cross-polarised with respect to laser transmission.

120 The ISP (Instrument Source Packets) generated by ATLID contain the measurement data as well as ancillary data such as number of accumulated shots, instrument mode, time information, laser frequency, laser energy, detector saturation, efficiency of the coalignment loop etc. ISPs are transmitted from the satellite to the PDGS, where the L0 data product is generated.

The ATLID ECGP (EarthCARE Ground Processor) is the L1 processor which ingests and processes the L0 files generated from the ISPs. At level 1, the main ATLID product is range-corrected attenuated backscatter signal that is the product between



EarthCARE JAXA L2 Production Model

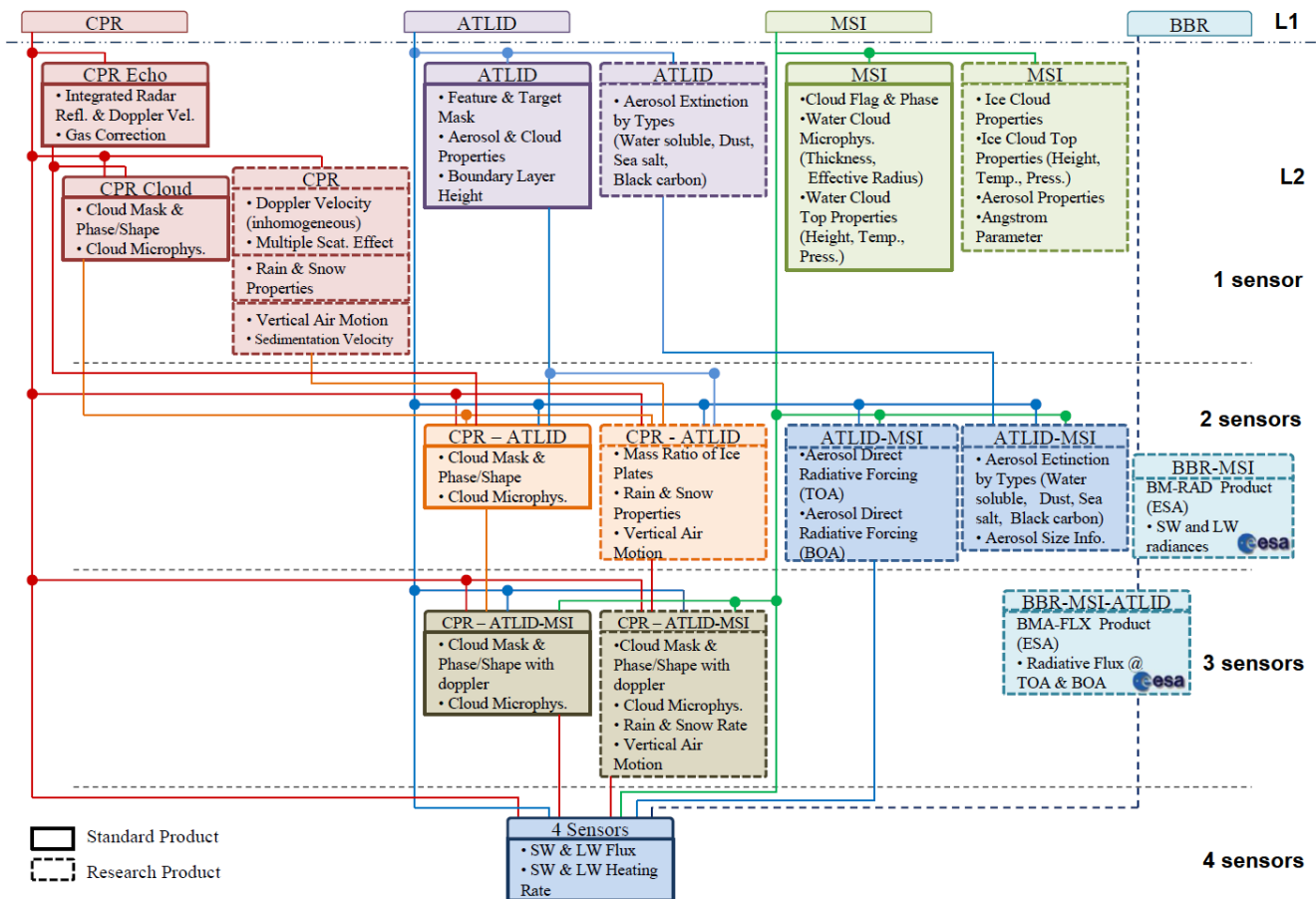


Figure 2. The JAXA "EarthCARE Production Model" shows all JAXA data products and ESA's level 1 and Aux products. Level 2 products and their retrieval algorithms (L2a, L2b) are described in this AMT Special Edition according to Table 2 (L2a) and Table 4 (L2b).

125 the backscatter coefficient and the round-trip atmospheric transmission versus altitude. Indeed, the signals at instrument output
 (i.e. at entrance of CCD) are a combination of the backscatter signals at instrument input (i.e the pure contribution from
 the atmospheric Mie co-polar, Rayleigh co-polar, and cross-polar optical power) after atmospheric effects. More precisely,
 the instrument output signals are linked to the input signal (after subtraction of the background) via a linear combination
 (which can be expressed in a matrix form) that describes the optical chain (transmissions of the different optical components,
 including cross-talks) and the detection chain. The major purpose of the L1 processor is to invert this matrix in order to retrieve
 130 the range-corrected attenuated backscatter signal. These variables will be contained in the nominal (L1B-NOM) products from
 EarthCARE. In addition, a number of L1 calibration products will be generated.



The L1 processor parameterisation relies on several CCDB (Characterization and Calibration Database) files, containing the processing parameters required by the processor and describing either the payload behaviour or the algorithm settings. 135 The CCDB is initially populated with data from ATLID on-ground characterisation and calibration. During flight it will be modified when necessary, updating parameters on the basis of on-orbit calibrations. The frequency of a parameter update extends from almost-fixed (for a number of on-ground characterised parameters) to regularly updated (for the outputs of the in-flight calibrations).

The ATLID modes of operation supported by the ECGP consist of the nominal lidar measurements (or NOM) interspersed 140 with different calibration operations:

1. **FSC: Fine Spectral Calibration:** consists of a fine frequency tuning of the laser around the current operational laser frequency, in order to minimize the spectral cross-talk on the Rayleigh channel. The optimal frequency is then selected for nominal measurements - performed once a week.
2. **DCC : Dark Current Calibration:** consists of measuring the frequency-resolved dark current on each channel, by 145 measuring the detectors signals while shutting-off the laser emitter - performed once a month.
3. **CSC : Coarse Spectral Calibration:** consists of tuning the frequency of the laser emitter (by relatively large frequency increments), in order to minimize the spectral cross-talk on the Rayleigh channel. A set of four to five optimal frequencies are chosen (the choice of the frequency is then done off-line with respect to other instrumental criteria) - performed at the beginning of life and when needed.

150 Therefore, the complete list of ATLID level 1b products is the following:

1. **A-NOM:** the nominal L1B-data : geolocated, calibrated range-corrected attenuated backscatter signal profiles, along with segregated-type associated errors and with intermediate products from the processing (raw signals, offset-removed signals, background-removed signals, energy-normalised signals and relative signals.)
2. **A-FSC:** the Fine Spectral Calibration products : optimal frequency and associated cross-talk, plus quality criteria (and 155 intermediate products : geolocation of the samples, raw signals and retrieved spectral cross-talks for each point.)
3. **A-DCC:** the Dark Current Calibration products : DSNU (Dark Signal Non Uniformity) maps for the three channels and associated errors and quality criteria (and intermediate calculations : geolocation of the samples, raw signals, offset as a function of vertical sample for each channel.)
4. **A-CSC:** the Coarse Spectral Calibration products : frequency of each (4 or 5) optimum point, the associated cross talks 160 (and intermediate products : geolocation of the samples, raw signals and retrieved spectral cross-talks for each point.)

The following sections describe the processing sequence.



3.1.1 Identification and counting of measurement data packets

Using ancillary data, the L1 processor identifies the packets that contain invalid raw data. The validity of these data has been assessed on-board during in-flight operations. The packets are accepted with respect to several criteria: supported instrument mode (measurement validity bit), emitted beam quality (spectral emission quality), control loop status (co-alignment emitter/receiver) detection health (background and signal saturation).

3.1.2 Geolocation

1. Range Evaluation Location: range information give the distance from the receiver for each echo sample. Range computations are independent of instrument mode and do not use measurement data stream, they rely only on the integration time and accumulation factor for the high (0 to 20km) and low (20 to 40km) resolution part of the echo signal and the computer clock.
2. Samples geolocation: satellite position, altitude and pointing data allow to perform geolocation of atmospheric echoes. The temporal attitude and orbital information is provided as auxiliary input files (line of sight is provided in a CCDB file) to the software that will compute the following steps for each profile time stamp :
 - Determination of position and attitude from time stamp;
 - Computation of line-of-sight targets;
 - Computation of geodetic coordinates of samples;
 - ECEF (Earth Centered Earth Fixed) frame to geodetic coordinates transformation.
3. Calculation of atmospheric parameters associated to the samples: using the geolocation information, atmospheric temperature and pressure are attributed to each sample by interpolation (spatial and temporal) of the ECMWF forecast data contained in the X-MET product. Besides delivering this information in the output product, these variables are used to calculate the effective Mie spectral cross-talk (contamination from the Rayleigh channel into the Mie channel) as the broadening of the Rayleigh backscatter depends on temperature and pressure profiles.

3.1.3 Radiometric pre-processing

1. Detector voltage offset correction: The signal offsets are continuously assessed and updated from detection raw data. These offsets come from the last analogue stage in the ATLID detection chain and are very slow varying perturbations of the detection signal, linked to laser transmitter thermal drifts. These offsets are evaluated in the first samples, before echo acquisition, and subtracted from the measurement.
2. Correction of dark signal non-uniformity: In this step, the dark signal is subtracted from the science data. The sample-resolved dark signal maps (Dark Signal Noise Uniformity (DSNU) maps) per channel are extracted from the last maps contained in the CCDB (i.e those produced during the last Dark Current Calibration (DCC) sequence).



- 195 3. Background subtraction: The background radiation needs to be subtracted from the atmospheric profiles. To do so, the background is measured just before (first sample) and after (last sample) echo acquisitions at each shot. A linear interpolation of both measurements is performed to retrieve background level in each vertical echo sample during acquisition. The background is then subtracted for each sample.
- 200 4. Laser energy normalisation: In order to mitigate the impact of laser energy fluctuation, a normalisation is performed. For this purpose, two reference energy levels are reference in the CCDB: a threshold energy as well as a reference energy. This normalisation is performed in two steps, (a) the mean energy over the accumulated shots is compared to the threshold energy (and the profile is discarded if lower than the threshold), (b) for the processed data, each profile is normalized by the reference energy.

3.1.4 Cross-Talk management

- 205 1. Cross-Talk analysis: There are a number of cross-talk parameters that should be considered: spectral cross-talk that is contamination of Mie channels into the Rayleigh, and vice-versa, plus polarisation cross-talk that is contamination between the co- and cross-polar channels. The objective of spectral cross-talk calibration is to compute cross-talk parameters that enable to retrieve, up to an absolute constant factor, Mie and Rayleigh scattering profiles from corrected raw signals delivered by the instrument. Absolute lidar constants, computed from on-ground absolute calibration process, must then be used to retrieve the input signal. Relevant information is contained in the CCDB. The initial cross-talk parameters are also computed on-ground during a specific calibration stage. In-flight calibration is carried out constantly during the measurements mode. This is performed in two successive steps:
- 210 (a) **Rayleigh spectral cross-talk** (contamination from the Mie into the Rayleigh channel). The baseline method for inferring the Rayleigh cross-talk value is to use ground echoes that can be assimilated as pure Mie signals (such as deserts or ice covers). Over these identified areas, the signals of the Rayleigh and Mie channels are averaged to reach a sufficient signal-to-noise ratio. The cross-talk value is then inferred by computing the ratio of Rayleigh and Mie channels. In order to increase the number of values, dense clouds are also used as determination targets.
- 215 The method is based on iteratively determining the cross-talk value leading to the smoothest path for the Rayleigh signal within the cloud. The cross-talk values are then interpolated along-track from these two series of anchor points.
- 220 (b) **Mie spectral cross-talk** (contamination from Rayleigh into the Mie channels). The method to infer the Mie cross-talk value relies on computing the ratio between signals (after radiometric pre-processing) on Mie channel and Rayleigh channel for high atmospheric layers (samples higher than 30 km of altitude). We suppose that at these high-altitudes, only Rayleigh scattering occurs (i.e., we have a pure Rayleigh spectrum). These signals are averaged along a determined number of samples along-track (estimation window) to reach a sufficient signal to noise ratio. The Mie cross-talk is a quantity which varies with altitude since molecular broadening is temperature and pressure dependent: the width of the Rayleigh signal varying with the atmospheric conditions, the proportion of Rayleigh



225 signal contaminating the Mie channel will then vary accordingly. To take that effect into account, the cross-talk
is first estimated at a reference altitude (at which a reference temperature is estimated) and the variation of the
cross-talk along the vertical axis is then computed from a 2-dimensional (T, p) look-up table as a function of
the temperature and pressure profiles interpolated from the X-MET product for each shot. The cross-talk values
are finally interpolated from the values determined in each estimation window. Following the same approach, the
230 Rayleigh and Mie channel lidar constants are determined in each window.

2. Channel demultiplexing. This part of the processing consists of three successive steps:

(a) Construction of the vertical profile of Mie cross-talk value: based on the Mie cross-talk value inferred at the pre-
ceding step, and its associated temperature, as well as the temperature-dependent variation law and the interpolated
temperatures of each vertical sample.

235 (b) Construction of the correction matrix for each sample: coefficients are combinations of spectral cross-talk coeffi-
cients, polarisation cross-talks (provided in CCDB) and lidar constants.

(c) Computation of the cross-talk corrected signals on the three channels and associated errors.

3. Physical conversion. The purpose of this processing is to retrieve pure range-corrected attenuated backscatter products.
Lidar absolute constants are applied to retrieve the absolutes signals from spectral cross-talk corrected instrument signals
and associated error products.
240

3.2 CPR

The CPR is a 94 GHz (W-band) cloud radar with Doppler capability that will provide cloud profiles, rain estimates and particle
vertical velocity. Raw instrument data (instrument science packets) as downlinked by the satellite are separated per instrument,
divided into frames of length 1/8 orbit, sorted in time, and stored together with a descriptive product header into level 0 data
245 products. Level 0 data is delivered from ESA PDGS to JAXA's EarthCARE mission operation system. This is then processed by
CPR level 1b processor which turns the raw data in engineering units into calibrated parameters, such as received echo power
and Doppler velocity, stored in level 1b data products. Geolocations, quality information, and error descriptors are added to the
level 1b products as well.

In CPR level 1b products, received echo power, radar reflectivity factor, normalized surface scattering cross section, Doppler
250 velocity, spectrum width, and data flag are included.

Gaseous attenuation corrected radar reflectivity factor, unfolded Doppler velocity and various cloud microphysical paramete-
rs are not included in level 1b and are processed in level 2a and 2b as shown in Section 5. CPR L1b processor makes the L1b
product for the data observed by Nominal observation mode, Contingency mode, and External Calibration mode. Invalid values
are stored under the effective observation altitude in the L1b product of Nominal observation mode. In the case of External
255 calibration mode, invalid values are stored in the region higher than 18km. The overview of the CPR L1b processor is described
in the following subsections.



3.2.1 Received echo power and Radar reflectivity factor

Received echo power (P_r) is converted from the log detector output of CPR level 0 data. It is integrated with about 500 m horizontal length on orbit. Mean P_r is calculated from division with integration number echo. Mean P_r is calibrated using receiver temperature and calibration load data (hot and normal). Received echo power is distributed before noise power subtraction in consideration of horizontal integration in level 2 processing. The vertical sampling window depends on the observation modes from -1.0 km below the ellipsoid model surface (WGS-84) to 16, 18 or 20 km above the ellipsoid surface for normal observation mode. Radar reflectivity factor (Z) is converted from Received echo power (P_r).

3.2.2 Normalized surface scattering cross section (NRCS)

The NRCS is the normalized radar reflectivity which corresponds to the land or ocean surface range. The NRCS is a radar cross section divided by the real cross section. Land and ocean surface range are inferred by surface estimation program written in section 3.2.5.

3.2.3 Doppler velocity

Doppler velocities represent vertical movement speeds of echoes if the beam direction of the CPR is precisely nadir. Doppler velocity is derived from IQ detector output instead of log detector output of CPR level 0 data. The echo phase angle ϕ is converted from the ratio of the real and imaginary parts of pulse-pair covariance coefficients. A phase change of transmit pulse ϕ_0 measured from leak signal to CPR receiver during transmit is used for collection of echo phase angle ϕ . Also, a phase correction ϕ_{sat} from satellite speed contamination to the radar beam direction V_{sat} is calculated from ancillary data (satellite velocity, attitude, beam direction). V_{sat} is calculated by dot product of the satellite velocity vector and the unit vector of CPR beam direction.

The Doppler velocity (V) is calculated as follows using ϕ , pulse repetition frequency PRF and wavelength λ :

$$V = \frac{\phi \times \lambda \times PRF}{4\pi}$$

The maximum ambiguity Doppler velocity, V_{max} , is defined as follows:

$$V_{max} = \frac{\lambda \times PRF}{4\pi}$$

Finally, vertical Doppler velocity from $-V_{max}$ to $+V_{max}$ is derived. Unfolding process and correction of non-uniform reflectivity effect is considered as level 2 processing (Section 5).

3.2.4 Surface estimation

Surface echo range is important for the higher level CPR algorithm. In L1b, surface echo range bin is determined using received echo power profile with the help of the digital elevation model information. Also, the exact location of the surface within a



285 pulse is calculated. In presence of drizzle and/or rainfall, CPR data suffers attenuation and the surface echo may disappear in heavy rainfall cases. This processing produces both the range bin information of the surface and the quality flag of the surface estimation.

3.3 MSI

The MSI (Wehr et al., 2023) embarks two cameras; the four channel VNS camera spanning Visible, Near Infrared and two
290 Short Wave IR bandwidths, plus the TIR camera with channels covering three Thermal IR bandwidths. These cameras produce the ISPs that are transmitted to the PDGS and processed to L0 data. MSI L1 processor ingests the MSI L0 product, along with data stored in MSI CCDB, to produce a number of products:

1. **M-NOM** – the nominal L1B data product with radiometrically calibrated imagery and auxiliary support data / quality metrics, including solar irradiance data;
- 295 2. **M-RGR** – the nominal L1C data product with radiometrically calibrated imagery, co-registered to TIR band 8, and auxiliary support data / quality metrics, including solar irradiance data;
3. **M-DRK** – containing all calibration products generated from VNS camera dark views;
4. **M-SD1** and **M-SD2** – containing all calibration products generated from VNS camera solar diffuser views (differentiated according to the diffuser used);
- 300 5. **M-BBS** – containing all calibration products generated during both the TIR cold-space and TIR calibration black-body views, which includes image statistics, auxiliary parameter statistics and also Failure Detection, Isolation and Recovery (FDIR) status flags;
6. **M-TRF** – containing statistical measurements of ancillary parameters that are involved in TIR sensitivity corrections, which data forms the references against which small deviations are assessed following each TIR CAL used for monitor-
305 ing for any long-term drifts.

3.3.1 Pre-processing

Data from both TIR and VNS channels has already been flat-fielded in the Instrument Control Unit on orbit, via subtraction of an offset that is collected during a regular on-orbit calibration. The flat-field compensates for detector dark current and gain. Initial scrutiny routines in the processor check the validity of the data stream, for instance for continuous error free data
310 and transmission, valid health flags, correct number of channels and sequence counts. Orbital night side data is not expected to contain VNS channels. Data from the TIR camera's three spectral channels must contain at least 19 Ground Lines (GL) of data, which is the Time Delay Integration (TDI) period for which the camera was calibrated on ground and which will be employed on orbit, as well as a channel obtained from reference areas on the 2-D detector. Some supplementary data is contained in a



TIR Auxiliary channel. The processor algorithms require to cover the TDI summing period in order to implement corrections
315 that use an average over reference area data. Discrete, VNS data channels can be processed independently of each other.

Processing MSI data to valid LIC also requires valid and continuous data over several seconds. The timing data from each
GL should differ from the previous one by the GL period of 63 ms. The channel of data that is generated by the Instrument
Control Unit (ICU) Auxiliary channel must be valid. If the data passes validity checks, then processing commences via one of
three streams, VNS processing, TIR processing or ICU auxiliary processing for the associated house-keeping telemetry.

320 3.3.2 VNS processing stream

VNS data has been corrected on orbit for gross offsets via the flat-fielding that is applied on orbit. Pre-processing first inverts
the image contrast, because unprocessed VNS signals decrease as light levels increase. The channel data is subtracted from a
display offset that is stored in the CCDB; by default it is the same for all four channels. An average is then calculated over
the wing pixel elements for each channel, these being non-illuminated pixels at both sides of each channel's 384 pixel wide,
325 linear detector array. For each channel, its wing element average signal is subtracted from every pixel sample to compensate for
detector dark offset drift and row correlated noise. Thus are generated four streams of VNS data in binary units, each of width
384 pixels (which includes the wing pixels), to which is attached a line specific quality metric and detector_temperature (both
from ICU ancillary data), plus the wing_sum (as computed). The four, channel wing-average signals are also made available to
the Instrument Calibration and Monitoring Facility (ICMF), for monitoring the health of the VNS detectors, where the average
330 signal can be correlated against the detector temperature recorded in the ancillary data.

The four streams of VNS data are then radiometrically calibrated into radiance values, with output expressed in $\text{Wm}^{-2} \mu\text{m}^{-1}$
 sr^{-1} . Appropriate radiance sensitivity data is selected from the CCDB. Conversion is a linear scaling operation using band-
specific and column-specific coefficients from the CCDB that cover all the illuminated columns of VNS data. Each illuminated
element in a stream of VNS data is multiplied by the calibration factor from the appropriate calibration factor array. The
335 conversion to spectral radiance must be performed before any re-sampling or interpolation involved with, for example, re-
sampling or re-mapping. The radiometric calibration must also be performed before any of the processing that is associated
with a VNS on-orbit calibration (every 16 orbits).

Calibration data is monitored, such that detector degradation and reduction in optical transmission can be compensated.
Correction factors for each pixel element in each band (a gain factor), based upon observations collected during the daily VNS
340 on-orbit calibration, will be updated periodically as part of the ICMF activity. The calibration maintenance gain factors form
part of a dedicated parameter set that is utilised by the ECGP.

VNS dark view calibration: This is collected with the aperture shut during the daily VNS calibration and upon any VNS
DAY procedure, which occurs following the dark side where VNS imagery is not collected. Radiance statistics are collected,
including average signal and temporal noise in each detector element, plus the associated detector temperatures, and form the
345 calibration product **M-DRK**.

VNS solar view calibration: This is collected at the daily VNS calibration view of the solar illuminated diffuser. The mean
solar irradiance and its standard deviation, accumulated for each illuminated column in each VNS band over the entire solar



exposure, as well as the solar SNR, are collected and stored in the calibration product **M-SD1** or **M-SD2**, according to which
diffuser was exposed. Data from the CCDB describing the scattering function of the diffuser as a function of detector column,
350 plus the solar illumination angles, are used to derive part of the product.

3.3.3 TIR processing stream

The TIR data stream is recovered from the 2-D TIR detector over a 384 column line width. Source channels 5 to 7 are allocated
to the three TIR spectral channels, source channel 8 is allocated to reference area data that is summed column-wise from 38
detector reference rows, plus a channel 9 for auxiliary data. The packets received from the three spectral channels have already
355 been subjected to Time Delay Integration (TDI) processing on-orbit (summing over several detector lines), so that each pixel
represents a spatial average over the last 19 ground lines. The reference area data has not been subjected to TDI, but is only
summed spatially over the 38 detector reference rows; it is used to correct for detector noise and small thermal drifts in the
relay lens structure that is viewed by the detector reference areas, over the time period of the TDI processing.

A TIR Display Offset, stored in the CCDB, is first subtracted from each column in the ground line (including reference
360 areas). At each new ground line a column correction must then be applied to the data from each spectral channel, using the
reference area data. To this end, at each ground line, the reference channel (which is the sum over 38 detector rows) is stored
in a buffer with 19 entries. The reference area temporal average is then computed for each column in the ground line, being the
sum of reference area signal in that detector column over the last 19 buffer entries, leading to a vector with 384 samples. The
column correction is applied to each TIR band element, subtracting the reference area signal in that column, with scaling for
365 the difference of the single spectral band ground line versus the 38-lines in the reference area.

After column correction an offset correction is applied, associated with the cold space mirror that is used for calibration
dark views. In case the ICMF has noticed a degradation associated with instrument sensitivities to certain parameters described
below, then sensitivity corrections could also be applied. The signal is then converted to brightness temperature measured in
Kelvin, according to band and column specific gain factors stored as look-up table in the CCDB.

370 TIR blackbody calibration: The gain factors used to convert TIR signal to brightness temperature should result in a Cali-
bration BlackBody (CBB) signal level that is in agreement with the temperature of the CBB that is very accurately measured
by precision thermometry during the daily on-orbit calibration. An initial set of gain factors is stored in the CCDB, measured
during the ground calibration campaign. The ICMF monitors the TIR transmission in each band and, if needed, generates a
new, time-stamped correction factor to be applied to all subsequent processing. The data product from the calibration is **M-BBS**
375 and it is used to generate the TIR gain correction factor.

TIR cold-space view calibration: Cold-space view statistics are collected during each daily, on-orbit calibration and will be
monitored at the ICMF. The Cold Space Mirror (CSM) offset correction that is applied to TIR data uses an array of column
specific offsets stored in the CCDB. A number of offset files have been generated, based on measurements made during the
ground calibration campaign along with calculations that consider a slow degradation of the mirror. Contamination of the cold-
380 space mirror used for the calibration dark view would cause a gradual signal drift. If it is judged to be too large then the drift



can be compensated for by selection of one of the alternative offset parameter files, in order to restore the correct baseline. The data product from the calibration is **M-BBS** and it is used to generate the associated TIR CSM offset factor.

Sensitivity corrections: During the TIR on-ground calibration, the sensitivity of the TIR camera to small perturbations of six parameters was tested, being TIR detector temperature, two TIR bias voltages VFID and VSKIM that relate to gain and offset settings, TIR relay lens temperature, TIR bench temperature and TIR cover temperature. The calibration involved modifying each of these parameters from the nominal set-point and measuring the camera response to hot and cold targets, in order to measure the offset and gain components at each detector column. Various TIR camera control systems (thermal, electrical, software) should prevent unacceptable deviations of these parameters, however, the processor will flag if any parameter exceeds its limit. Statistical measurements of relevant ancillary telemetry collected during cold space views is stored in the **M-TRF** data product. The ICMF has the option to impose sensitivity corrections as additional gain and offset parameters, computed using TIR calibration data, however the initial processor configuration does not apply any sensitivity corrections. In case it is required that sensitivity correction(s) is/are imposed, they are applied line by line to the column corrected TIR image data using sensitivity vectors and ancillary parameters from the current line and last TIR calibration.

NB: TIR temperature to radiance and radiance to temperature transforms: Any interpolation operation on TIR data, for instance for co-registration to L1c, must be applied to radiance values, never to TIR brightness temperature, and the CCDB contains the associated look-up tables. One set of look-up tables contains band specific tables relating the TIR brightness temperature to radiance, for each of the three bands, at a resolution one tenth of the best case NEdT. The band specific inverse transformation tables for radiance to brightness temperature conversions are also supplied. The conversion tables should only be applied to radiometrically calibrated data.

400 **3.4 BBR**

The BBR is a radiometer that will measure the Total Wave (TW) and reflected Short Wave (SW) radiation from the Earth scene, from which information concerning the emitted Long Wave (LW) is also derived. It collects data in three directions, forward, nadir and aft along track via three different telescopes. A chopper drum with four apertures - two of which house 2 mm thick, curved, quartz filters for filtering of the longwave radiation (i.e to measure the Shortwave only) - rotates continuously around the telescopes, chopping the signal onto the detectors through the sequence SW, drum skin, TW, drum skin etc.

A Calibration Target Drum rotates around the Chopper Drum. The different calibration targets are : hot and cold blackbodies, a sun-diffuser, three fold mirrors and the telescope baffles. the fold-mirrors function is to be able to observe the diffuser from each telescope. Approximately every 80 s the telescopes' views are directed onto a hot or cold black body. SW calibration is performed every two months, by accumulating views of the sun illuminated diffuser over approximately 30 orbits. Monitor Photo Diodes in the telescope baffles allow aging of the Visible Calibration system (VisCal) to be assessed.

The level 1 processing aims at providing unfiltered radiances over various geographical scales within two products that are elaborated hereunder. However, the user is advised that these products are not directly suitable for science applications, because the instrument effects are not fully removed. Instead, the user is advised to use the (so-called unfiltered) product BM-RAD:



1. **B-NOM** – the nominal BBR products averaged over various geographical scales:

- 415
- standard product: averaged over 10 km along-track and 10 km across-track using a trapezoidal weighting function of the Point Distribution Function (PDF).
 - small product: averaged over 10 km along-track and 5 km across-track using a rectangular weighting function of the PDF.
 - full product: averaged over 10 km along-track and over the full range of the product across-track.

420 2. **B-SNG** – the single pixel product in which the filtered radiance is provided at the pixel-resolution.

The ECGP algorithm has three processing steps. Step 1 operates on the incoming ISP (Instrument Source Packets), encapsulated as the L0 product. Step 2 annotates the incoming per-telescope data with the correct gains and offsets to apply derived from the calibration sequences. Two ageing (calibration) products are output from this stage:

- 425
1. **B-SOL** – the solar calibration BBR L1 product. The BBR Solar Calibration data product is a collection of the SW ageing views over time.
 2. **B-LIN** - the linear calibration BBR L1 product. The BBR Linear Calibration data product is a collection of the measured gain (and offset) while viewing the blackbodies (BBs) during a linearity check.

Step 3 takes each data stream (one per telescope) and performs the radiometric corrections and the various spatial summations to generate the measurement level 1 products: B-NOM and B-SNG. These three steps are described further hereafter.

430 3.4.1 Marshalling stage

The processed ISPs from BBR are arranged in the L0 chronologically with 24 acquisitions (8 per telescope), per ISP. This stage takes the L0 product and rearranges the data as an acquisition stream per telescope. At this stage, the relevant house-keeping (HK) and satellite information is annotated into the data. The sequence is:

- 435
- Output an intermediate file per ISP containing the measured resistance temperatures (using current/temperature Look Up Tables) per telescope, along with black-bodies and instrument temperatures.
 - Quality check: check if a corrupted flag has been raised or if data are insufficient within one ISP (reject if so). An additional flag is potentially raised per pixel based on the generated voltage quality check (to highlight high contrast scenes at pixel level).
 - Annotate the ISP with the exposure type: the calibration drum position, to designate Total Wave, Short Wave or a View of the drum inner surface (if the position differs for two successive acquisitions then the drum is considered as moving for the first acquisition which is flagged as invalid).
 - Annotate the ISP with the spacecraft position and pointing observation.
- 440



- Generate an intermediate file of telescope (i.e. three files) data based on the incoming values.
- Generate an intermediate file of the output values of the monitoring photodiodes, when relevant (i.e when a visible calibration is performed) along with the concerned telescope.

445

3.4.2 Radiometric calibration

At this stage, the incoming per-telescope data are annotated with the gains and offsets to apply, derived from the calibration sequences. The geo-location information are also added. Preliminary radiometric corrections are performed and the two calibration products are generated at this stage.

- 450 – Chopper subtraction: the background radiation generated by the chopper drum is subtracted from the voltage measured for each acquisition.
- Geolocation: The first operation is to create the ground positions (along-track) representing the pixel barycentres. This is derived from the spacecraft attitude data by computing the intersection of the line of sight using the EOCFI dedicated routines. Secondly the ground coordinates are derived for each of the measurement pixels. Finally these are also translated into along-track and across-track coordinates with respect to the barycentre ground-track. All these information are annotated to the telescope files.
- 455
- Gain calculation: this calibration processing is performed on a telescope-by-telescope basis. It consists of determining the gains and offsets for the TW and SW channels for each telescope. For a given calibration sequence, typically four measurements (two TW and two SW) of each internal blackbodies (hot and cold) are performed. After averaging over the available measurements in the sequence, two values are derived, being, the voltages TW and SW for each blackbody (these values are corrected from the dark current). The radiance of each black body is then interpolated in a two-dimensional look-up table (dependent on blackbody and telescope temperatures) using the intermediate file created during the marshalling stage. Offsets for SW and TW channels are directly given by the voltages measured for the cold blackbody. The TW gain is given by the ratio of the difference of voltage for hot and cold BB and the difference of radiance for the two BBs. Finally, the SW gain is obtained by multiplication of the TW gain by the SW Gain Ratio (value is extracted from the CCDB). This ratio is first characterized on ground but is affected by the ageing of the quartz filter. For this reason it is regularly updated during the solar measurement (VisCal). These calibration values are stored in the B-LIN which is produced at this stage.
- 460
- Output B-SOL: this stage parses the telescope file to generate the calibration file corresponding to the SW calibration position (once per orbit) which contains acquisition time, sun position, signal levels on the three telescopes (both when the SW filter is in place and not), gains and offsets information, as well as quality information. This data is used, following careful inspection by the ICMF, to assess if there is any ageing of the SW spectral response. If this this is the case, the SW Gain Ratio parameter will be modified accordingly.
- 465
- 470



3.4.3 Integrate and create products

475 For the B-NOM product, the following processing sequence is applied: first a list of product barycentre is produced at a 1 km
interval (the processor determines what the barycentres location should be with respect to the along-track pixel positions).
Then for the three different resolutions of the product (standard, small, full) it is determined from the along-track dimension,
which pixels are to be integrated in the product. Conversion of along-track/across-track into geodetic latitude/longitude is also
performed. Depending on the associated weighting function (dependent on the product resolution), a weight is then associated
480 to each individual pixel. After correction of the offset and the gain for each channel (TW and SW), the integration of the
weighted product is performed over the pre-determined area for each resolution. The LW radiances are then derived from the
subtraction of the SW radiances from the TW ones, keeping in mind the differential gain of the channels.

For the B-SNG product, the gain and offset corrected radiances are provided at pixel level and for the TW and SW channels
(no LW radiances are derived).

485 4 Auxiliary data (level 1d) processors and products

4.1 X-MET: Meteorological fields for the EarthCARE swath

The X-MET processor generates the EarthCARE meteorological product, X-MET, using meteorological fields selected from
output of the ECMWF Early Delivery System of the Atmospheric Model high-resolution 10-day forecast (HRES) model
and sub-setting them to the EarthCARE swath while keeping them on the original model grid. This reduces significantly the
490 data volume as compared to using global meteorological fields (reduction by a factor 20) or as compared to interpolation to
EarthCARE instrument grids or the EarthCARE Joint Standard Grid.

The X-MET product format is compliant with the generic EarthCARE product format and EarthCARE metadata conven-
tions. It includes certain derived parameters, being tropopause height (both for the World Meteorological Organisation (WMO)
and CALIPSO definitions) and wet bulb temperature. The X-MET swath is based on the EarthCARE ideal orbit and includes
495 an allowance for the dead band, within which the actual orbit is maintained.

X-MET products are generated four times per day, according to the production schedule of ECMWF Early Delivery data by
its Integrated Forecast System (IFS). Each production run covers about 20 hourly forecasts, which, considering EarthCARE
1/8 orbit granularity, corresponds to 104 X-MET products per run. This generally results in multiple X-MET products being
available for any selected time.

500 Horizontal grid: Parameters are provided on ECMWF model grid points, which is a reduced Gaussian grid. ECMWF uses
an octahedral grid, with a resolution between 8 and 10 km, and a total number of 6.59 million grid points. However, only grid
points within a 330 km swath around the EarthCARE ground track are included in X-MET, leading to about 26,900 grid points
per frame.

Vertical grid: Pressure and geometric altitude on model levels are provided in X-MET for each point of the horizontal grid,
505 which enables interpolation/conversion from model levels to pressure or altitude coordinates. Unlike other EarthCARE data



products, which have the lowest altitude level at or below the Earth reference ellipsoid independent of the topography, for X-MET, lowest altitude level is the actual surface level, i.e. it follows the topography.

Should the ECMWF model resolution change in the future, X-MET will follow, i.e., it will always be provided at the original model resolution.

510 Grid point coordinates (latitude, longitude, altitude) are provided within the X-MET product. Parameters in X-MET are interpolated linearly between two adjacent forecasts (or the analysis and the first forecast) to a representative EarthCARE sampling time (mid-time of the frame). The temporal sampling of the forecasts between which this interpolation takes place is one hour. As X-MET contains data interpolated in time to the EarthCARE sampling time, processors using X-MET do not need to interpolate in time, only in space. Relevant times are reported in the Specific Product Header.

515 The X-MET processor runs inside a Kubernetes cluster on a platform provided at ECMWF, with access to the output from their HRES model. It will be managed and monitored by ECMWF, whilst the pods - containers with shared storage and network resources, used to transfer the X-MET product - will be managed by the PDGS.

4.2 X-JSG: The Joint Standard Grid

This processor creates the EarthCARE Joint Standard Grid product, X-JSG, from the geolocation in ATLID and CPR level 1b products. X-JSG contains the common spatial grid used across instruments in EarthCARE level 2 processing, called Joint Standard Grid, and a number of additional geolocation parameters widely used in level 2 processing; a land flag, terrain elevation, solar angles, viewing angles and some index and count parameters. X-JSG itself does not contain any instrument observation data. It ensures that the data from radar, lidar and multispectral imager can be collocated such that they are observing the same column of the atmosphere. The X-JSG level 1d grid product consists of two, two-dimensional (2D) grids, creating a three dimensional grid that follows the EarthCARE track. X-JSG is constructed by combining:

- The CPR horizontal grid along track (combining two CPR pixels for every JSG pixel, or approximately 1 km),
- The ATLID vertical grid, and
- A fixed 1 km grid to extend the grid across track to cover the complete MSI swath.

In case of non-availability of either CPR or ATLID measurement data, the X-JSG processor falls back to a contingency solution. This is implemented, for instance, during instrument calibration modes. In such instances the grid will be constructed without the respective instrument, using a similar but fixed sampling. In case of non-availability of both CPR and ATLID measurement data for a complete frame, no JSG will be produced. However, in such instances synergistic retrievals, without measurements from the active sensors, are not required. The horizontal grid point locations define the X-JSG pixel centres. Pixels across track, for a given along-track position, share the same vertical grid. The vertical grid is specified for each grid point along track, as the position of the vertical grid points varies along track due to the dynamic adaptation of the ATLID range to the satellite height, combined with a finite step size for the range.

Along track: The spatial extent of the along-track grid is equal to a frame (1/8 orbit), which is the granularity of all EarthCARE products. However, the CPR creates profile groups of 14 CPR profiles, between which there is a larger spacing, which



540 results in a series of seven X-JSG pixels. The nominal X-JSG grid is irregular due to this way of CPR sampling. In case of no CPR measurement data, X-JSG will use a fixed 1000 m horizontal grid point distance (configurable).

Across track: Set via a configuration that defines a fixed 1 km grid sampling and the left and a right boundary dimensions, selected based on MSI sampling and swath size.

545 Vertical: Vertical grid point distance is defined by ATLID vertical sampling, which is about 103 m up to an altitude of 20 km and 500 m above this altitude. The lower and upper boundaries of the vertical grid are set via configuration parameters. In case of no ATLID measurement data, a vertical grid is created with two possible vertical grid point sample distances, high-resolution at 100 m sample distances and low-resolution at 500 m vertical sample distances. The high and low resolution sample distances, as well as the altitude boundary of these sampling regions, are configurable.

550 This product facilitates the application of synergistic (L2b) classification and retrieval algorithms as well as the synergistic use of a number of single-instrument (L2a) products. It is closely linked to the merged observations product (AM-MO) which directly uses the JSG definition in order to produce a file containing co-located observations.

5 Level 2 data processors and products

EarthCARE level 2 data products include a comprehensive range of geophysical parameters related to aerosols, clouds, precipitation and radiation. Wehr et al. (2023) (section 8.3) give an overview of the ESA and JAXA L2a/L2b data products containing retrieved aerosol, cloud, precipitation and radiation parameters and supporting science activities. In this section we provide 555 brief descriptions of all level 2 data products and references to corresponding publications which contain detailed information about the products, retrieval algorithms and their verification and validation. Tab. 1 and 2 lists all ESA and JAXA level 2a (L2a) data products, i.e., data products derived from one EarthCARE instrument only, along with the reference for their detailed description. Data products synergistically retrieved from more than one EarthCARE instrument are referred to as level 2b (L2b) data products. Inputs to L2b processors may be L1b/c/d data products as well as L2a and other L2b data products. Tab. 3 560 and 4 lists all ESA and JAXA L2b data products including their respective reference. All products listed in Tab. 1 and 3 are operationally produced by the ESA PDGS. For products listed in Tab. 2 and 4, Standard Products are operationally produced by the JAXA Satellite Applications and Operations Center (SAOC), while Research Products are products by JAXA Earth Observation Research Center (EORC) and/or Japanese institutes/universities. All products will be made available to users usually not later than 48 hours after sensing.

565 While not part of the ESA or JAXA data products, the development of a cloud climate product processor for ATLID is relevant in this context. It is designed with the purpose of making ATLID cloud observations directly available for climate applications (Feofilov et al., 2023).



5.1 Single-instrument (level 2a) processors and products

5.1.1 ESA single-instrument processors and products

570 ESA data products generated from measurements of a single instrument are listed in Table 1. There is no BBR level 2a product, as scene information from the MSI is required to derive radiances and fluxes from BBR. Level 2a products are usually provided at instrument resolution or multiples thereof, ATLID and CPR on a vertical “curtain” (dimensions: along track and altitude), and MSI on a horizontal “swath” (dimensions: along track and across track).

For each of the active instruments, ATLID and CPR, two classification products are produced, a feature detection mask that provides areas of significant return (A-FM and C-FMR) and a target classification that identifies various classes of hydrometeors and aerosols (A-TC and C-TC). From the radar reflectivity corrected for gaseous attenuation and non-uniform beam filling (also in C-FMR), and Doppler velocities corrected for antenna mispointing, non-uniform beam filling and velocity folding (C-CD), are derived vertical profiles of cloud and precipitation microphysical parameters (C-CLD). The primary ATLID level 2a product contains vertical profiles of extinction, backscatter and depolarisation (A-EBD). This is the starting point for further ATLID products covering aerosol profiles (A-AER), ice cloud profiles (A-ICE) and layer information for clouds (A-CTH) and aerosols (A-ALD).

Level 2 processing for MSI starts with a classification product as well (M-CM). This contains the cloud flag, cloud phase and cloud type. In a second stage, cloud optical and physical properties, namely cloud optical thickness, effective radius and top height are derived (M-COP), as well as aerosol optical thickness (M-AOT).

5.1.2 JAXA single-instrument processors and products

Table 2 shows all JAXA L2a products and their product category shown in the JAXA Production Model in Figure 2. Short descriptions of the JAXA L2a products are as follows:

CPR_ECO – containing 1 km and 10 km horizontally integrated radar reflectivity and Doppler velocity. Clutter echo correction and gas attenuation correction are provided for radar reflectivity, and Doppler unfolding correction is provided for the Doppler velocity.

CPR_CLP – containing cloud mask, cloud particle type and cloud microphysics, which are derived mainly from radar reflectivity factor.

ATL_CLA – providing classification for each ATLID observation grid and optical properties of cloud and aerosol such as extinction coefficient, backscatter coefficient, lidar ratio, and depolarisation ratio. Planetary boundary layer height is also contained.

MSI_CLP – cloud product derived from MSI, including cloud flag and phase information and water cloud properties such as effective radius and optical thickness. Furthermore, cloud top temperature, pressure and height are provided. Ice cloud properties are in MSI_ICE product.

CPR_DOP – the corrected Doppler velocity, considering inhomogeneity and unfolding is included, in addition to the correction for Doppler velocity performed in CPR_ECO.



Product Name	Processor Name	Derived from instrument	Content	Reference
C-FMR C-CD C-TC	<i>C-PRO</i>	CPR	Feature mask and corrected reflectivity Corrected Doppler Target Classification	Kollias et al. (2023) Kollias et al. (2023) Irbah et al. (2023)
C-CLD	<i>C-CLD</i>	CPR	Cloud profiles	Mroz et al. (2023)
A-FM	<i>A-FM</i>	ATLID	Feature mask	van Zadelhoff et al. (2023)
A-AER A-ICE A-TC A-EBD	<i>A-PRO</i>	ATLID	Aerosol profiles Ice water content and effective radius Target classification Extinction, backscatter, depolarisation	Donovan et al. (2023b) Donovan et al. (2023b) Irbah et al. (2023), Donovan et al. (2023b) Donovan et al. (2023b)
A-CTH A-ALD	<i>A-LAY</i>	ATLID	Cloud top height Aerosol layer descriptor	Wandinger et al. (2023) Wandinger et al. (2023)
M-CM M-COP	<i>M-CLD</i>	MSI	Cloud mask and phase Cloud optical and physical properties	Hünerbein et al. (2023b) Hünerbein et al. (2023a)
M-AOT	<i>M-AOT</i>	MSI	Aerosol optical thickness	Docter et al. (2023)

Table 1. References of all ESA L2a products and their retrieval algorithms shown in the ESA Production Model, Figure 1.

CPR_RAS – providing parameters related to rain and snow, such as rain water content, snow water content, ratio rate, snow rate. Attenuation corrected radar reflectivity is also contained. Two types of rain water content and snow water content, with and without Doppler velocity, are available.

CPR_VVL – containing vertical air motion in cloud regions and sedimentation velocity of cloud particles.

605 ATL_ARL – extinction coefficients for four aerosol components (dust, black carbon, sea-salt and water-soluble particles) are included.

MSI_ICE – including optical thickness, effective radius and cloud top temperature/pressure/height of ice cloud. Water cloud properties are in MSI_CLP product.

610 MSI_ARL – aerosol optical thickness and Angstrom exponent derived from MSI are contained. Angstrom exponent is available only over ocean.



Product Name	Product Category	Derived from instrument	Content	Reference
CPR_ECO	Standard	CPR	Radar reflectivity and Doppler velocity	Hagihara et al. (2021)
CPR_CLP	Standard	CPR	Cloud mask/type and cloud optical properties	Hagihara et al. (2010), Kikuchi et al. (2017), Okamoto et al. (2010), Sato and Okamoto (2011), Okamoto (2023)
ATL_CLA	Standard	ATLID	Feature mask, target mask, and cloud/aerosol optical properties	Nishizawa et al. (2019); Nishizawa (2023); Hagihara et al. (2010); Yoshida et al. (2010); Oikawa (2023)
MSI_CLP	Standard	MSI	Cloud flag/phase and water cloud properties	Nakajima et al. (2019), Wang et al. (2023)
CPR_DOP	Research	CPR	Doppler velocity correction value and unfolding value	Hagihara et al. (2021); Hagihara (2023)
CPR_RAS	Research	CPR	Rain/Snow water content, Rain/Snow rate	Sato et al. (2009); Sato (2023)
CPR_VVL	Research	CPR	Vertical air motion and sedimentation velocity	Sato et al. (2009); Sato (2023)
ATL_ARL	Research	ATLID	Aerosol extinction coefficient of water soluble, dust, sea salt, and black carbon	Nishizawa et al. (2008, 2011)
MSI_ICE	Research	MSI	Ice cloud properties	Letu et al. (2016, 2018)
MSI_ARL	Research	MSI	Aerosol optical thickness and Angstrom exponent	Yoshida et al. (2018)

Table 2. References of all JAXA L2a products and their product category shown in the JAXA Production Model, Figure 2.

5.2 Synergy (level 2b) processors and products

5.2.1 ESA synergy processors and products

ESA data products generated from measurements of two or more EarthCARE instruments are listed in Table 3. Level 2b products are usually provided on the Joint Standard Grid described in section 4.2.



The single-instrument target classifications (A-TC and C-TC) are used to derive a synergistic target classification (AC-TC). Synergistic ATLID/MSI layer products are generated for clouds (AM-CTH) and aerosols (AM-ACD). The primary synergy product for cloud, aerosol and precipitation parameters is ACM-CAP, which uses an optimal estimation scheme. In addition, and as a backup for ACM-CAP, a simpler synergy product ACM-COM contains a best estimate of cloud and aerosol profiles
620 based on a composite of level 2a products. As a preparation to the radiative transfer calculations, a three-dimensional scene is constructed finding nadir pixels that match off-nadir pixels in MSI radiance (ACMB-3D). In this way, the cloud, aerosol and precipitation fields from ACM-CAP (or as a backup, from ACM-COM) can be extended out to 15 km across-track and used in 1D and 3D radiative transfer models to derive broadband radiances, fluxes and heating rate profiles (ACM-RT). Broadband radiances (BM-RAD) and fluxes (BMA-FLX) are also derived directly from BBR measurements. In a final assessment step
625 (ACMB-DF), broad-band radiances and fluxes from radiative transfer models are compared to the ones from BBR.

5.2.2 JAXA synergy processors and products

Table 4 shows all JAXA L2b products and their product category shown in the JAXA Production Model in Figure 2.

Short descriptions of the JAXA L2b products are as follows:

AC_CLP – similar parameters as CPR_CLP are estimated using CPR-ATLID, however, the number of grids with valid values
630 increases compared with CPR_CLP because AC_CLP is derived from both CPR and ATLID, which have different sensitivity for thin and deep clouds.

ACM_CLP – similar parameters as CPR_CLP and ACM_CLP are estimated using CPR-ATLID-MSI. In addition, liquid water path and ice water path are available in ACM_CLP.

ALL_RAD – containing radiative fluxes and heating rate for both shortwave and longwave regions derived with 1D plane-
635 parallel radiative transfer simulation.

AC_MRA – containing two types of mass ratio of 2D ice to ice water content. One is derived with Doppler velocity and the other without Doppler velocity.

AC_RAS – providing rain water content, snow water content, rain rate and snow rate, derived utilising both CPR and ATLID data. Two types of rain water content and snow water content, with and without Doppler velocity, are available.

640 AC_VVL – providing information related with atmospheric vertical motion estimated with CPR and ATLID data. The parameters of vertical air motion and sedimentation velocity are included.

AM_ARL – providing extinction coefficient of each aerosol type (dust, black carbon, sea-salt, and water-soluble particles) and mode radius for fine mode and coarse mode. Aerosol direct radiative forcing at Top Of Atmosphere (TOA) and Bottom Of Atmosphere (BOA) are included as well.

645 ACM_CDP – containing cloud mask, cloud particle type, liquid/ice water path and cloud microphysics derived from ATLID, CPR and MSI data. ACM_CDP utilizes Doppler velocity.

ACM_RAS – containing same parameters as AC_RAS, but ACM_RAS is derived from three sensors of ATLID, CPR and MSI.



Product Name	Processor Name	Derived from instruments	Content	Reference
AM-CTH	<i>AM-COL</i>	ATLID, MSI	Cloud top height	Haarig et al. (2023)
AM-ACD			Aerosol column descriptor	Haarig et al. (2023)
AM-MO	<i>AM-MO</i>	ATLID, MSI	ATLID & MSI level 1b merged onto same grid	
BM-RAD	<i>BM-RAD</i>	BBR, MSI	Broad-band radiances (unfiltered)	Velázquez Blázquez et al. (2023a)
BMA-FLX	<i>BMA-FLX</i>	BBR, MSI, ATLID	Broad-band fluxes	Velázquez Blázquez et al. (2023b)
AC-TC	<i>AC-TC</i>	ATLID, CPR	Synergistic target classification	Irbah et al. (2023)
ACM-CAP	<i>ACM-CAP</i>	ATLID, CPR, MSI	Cloud, aerosol, precipitation best estimates	Mason et al. (2023b)
ACM-COM	<i>ACM-COM</i>	ATLID, CPR, MSI	Composite cloud and aerosol profiles	Cole et al. (2022)
ACMB-3D	<i>ACMB-3D</i>	ATLID, CPR, MSI, BBR	Constructed three-dimensional scene	Qu et al. (2023)
ACM-RT	<i>ACM-RT</i>	ATLID, CPR, MSI	Radiative transfer products - fluxes, radiances, heating rates from 1D and 3D models applied to retrieved cloud/aerosol/precip scenes	Cole et al. (2022)
ACMB-DF	<i>ACMB-DF</i>	ATLID, CPR, MSI, BBR	Differences between radiances and fluxes calculated from retrievals (ACM-RT) and BBR measurements (BM-RAD, BMA-FLX)	Barker et al. (2023)

Table 3. References of all ESA L2b products and their retrieval algorithms shown in the ESA Production Model, Figure 1.

ACM_VVL – containing same parameters as AC_VVL, but ACM_VVL is derived from three sensors of ATLID, CPR and
 650 MSI.

ACM_ICE – containing effective radius and optical thickness of ice cloud derived with the emission method called MWP method (Multi-wavelength and multi-pixel method).



Product Name	Product category	Derived from instruments	Content	Reference
AC_CLP	Standard	ATLID, CPR	Cloud mask/type and cloud optical properties	Okamoto et al. (2007, 2008, 2010), Hagihara et al. (2010), Kikuchi et al. (2017), Sato and Okamoto (2011)
ACM_CLP	Standard	ATLID, CPR, MSI	Cloud mask/type and cloud optical properties	Okamoto (2023)
ALL_RAD	Standard	ATLID, CPR, MSI, BBR	SW/LW radiative flux and radiative heating rate	Oikawa et al. (2013, 2018), Okata et al. (2017), Yamauchi (2023)
AC_MRA	Research	ATLID, CPR	Mass ratio (2D Ice/IWC)	Sato et al. (2009); Sato (2023)
AC_RAS	Research	ATLID, CPR	Rain/snow water content and rain/snow rate	Sato (2023)
AC_VVL	Research	ATLID, CPR	Vertical air motion and sedimentation velocity	Sato et al. (2009); Sato (2023)
AM_ARL	Research	ATLID, MSI	Aerosol extinction coefficient of water soluble, dust, sea salt, and black carbon, mode radius	Kudo et al. (2016)
AM_ARL	Research	ATLID, MSI	Aerosol direct radiative forcing	Oikawa et al. (2013, 2018)
ACM_CDP	Research	ATLID, CPR, MSI	Cloud mask/type and cloud optical properties with Doppler velocity	Okamoto (2023)
ACM_RAS	Research	ATLID, CPR, MSI	Rain/snow water content and rain/snow rate	Okamoto (2023)
ACM_VVL	Research	ATLID, CPR, MSI	Vertical air motion, sedimentation velocity	Okamoto (2023)
ACM_ICE	Research	ATLID, CPR, MSI	Ice cloud optical properties with emission method	Okamoto (2023)

Table 4. References of all JAXA L2b products and their retrieval algorithms shown in the JAXA Production Model, Figure 2.



6 Development of the EarthCARE processing chain

6.1 End-to-end simulator E3SIM

655 Development and test of the processors was made possible using a dedicated EarthCARE End-to-End Simulator (E3SIM).
 Test data, consisting of input scene files that describe the physical properties, were assembled by assimilation of data from
 many sources. Forward models were used to operate on the input scene files and generate the expected input to each of the
 instruments, with instrument models to simulate the engineering data that would be output from the instruments and transmitted
 to the ground. The L0, L1 and L2 processors could then be used to generate the corresponding data products, which need to be
 660 compared against the input data. The E3SIM is optimised for producing small amounts of highly representative data to be used
 in algorithm development. It is not meant to be used for routine operational generation of data products.

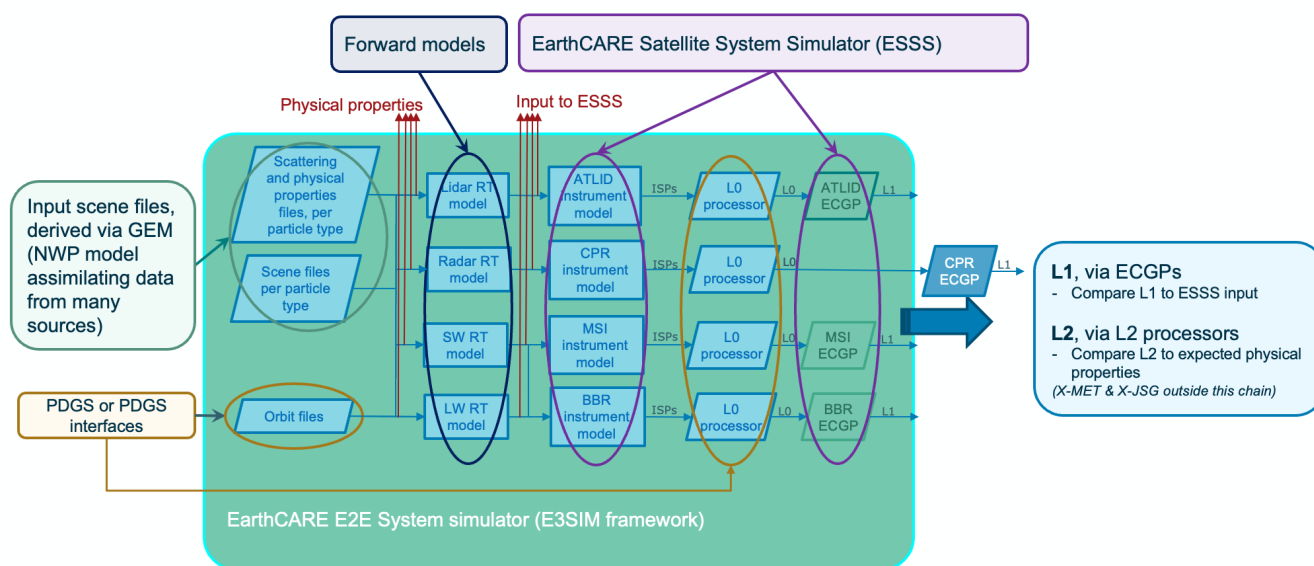


Figure 3. Simulation chain developed for the EarthCARE processors development. RT=Radiative Transfer, SW=Short Wave, LW=Long Wave, NWP=Numerical Weather Prediction, E2E=End to End, ECGBP=EarthCARE Ground Processor

E3SIM consists of the simulator framework, which allows to configure and run simulations of the complete processing chain or any part of the chain (down to individual processor runs), and the individual processor modules that are plugged into the simulator. Processors are connected to each other via their products and outputs of one processor in the chain are inputs to one
 665 or more processors further down in the chain. The production model (Figure 1) is implemented via “task tables”, which describe the inter-dependencies between processors in a general way. From these, “job orders” are generated as the basis for specific production runs, listing all required input data for a given run. This interface is the same as the one used by the operational PDGS, simplifying the development and testing as the processors have to support only a single interface.



6.2 Test data sets

670 The E3SIM was used to generate a number of test data sets for the processor development. Test data for level 1 processor
verification used scenarios from the EarthCARE system requirements wherever possible. These typically cover the extremes
of dynamic ranges, from detection limit to saturation. Level 2 processors used a wide range of input scenes, from simple
synthetic scenes in the early stages of development, via scenes based on campaign data and satellite measurements, specifically
the A-train instruments CloudSat, CALIPSO and MODIS, to the three science reference frames, Halifax, Baja and Hawaii,
675 based on the Canadian numerical weather prediction model, GEM. This dataset and its generation are described in detail by
Qu et al. (2022) and Donovan et al. (2023a). It covers a wide range of cloud and aerosol scenes and was used extensively in
the development, verification, and inter-comparison (Mason et al., 2023a) of the EarthCARE level 2 processors.

A dataset from a global storm-resolving simulation, and its use in the global evaluation of CPR Doppler velocity errors, is
described by Roh et al. (2023) and Hagihara et al. (2023).

680 6.3 Collaborative development

The large number of data processors and processor developers, and the complex production model with its many inter-
dependencies, required an efficient setup for enabling collaboration between developers, sharing code and information, testing
and managing software problems. We used a highly integrated, collaborative software development environment, based on a
mix of proprietary and open source tools such as Atlassian Confluence for sharing information and minutes of meeting, Atlas-
685 sian JIRA for reporting software problems and planning work, gitea as a code repository, Jenkins for running automated tests,
and MinIO as a test data repository.

6.4 Lessons learnt

After more than 15 years of developing the EarthCARE processing system, it is useful to look back and reflect on what could
have been done better and what worked well.

690 We found that it is important to systematically build up the end-to-end simulation chain and keep it consistent along the
way. Interfaces and reference software environments should be defined and documented very early. It is useful not to develop
everything in parallel from the start, instead to build a single chain first (preferably the one for the “simplest” instrument), then
review what can be improved, feed that into general requirements, and apply the lessons learned to remaining chains (which
can then be done in parallel). Level 1 processors need to be connected to the level 2 processing chain early.

695 Consistency of the simulation and processing chain (including input data) should be verified regularly. Late (fundamental)
changes in the processing chain must be avoided. If they do happen, they must include a corresponding adaptation of other
parts of the chain to keep it consistent (example: level 1 processor update might require an instrument simulator update).

Expertise and developments should be organised “vertically” along instrument processing chains (e.g. ATLID, CPR), rather
than “horizontally” along processing levels (e.g. instrument simulator, level 1 processor).



700 Test data sets should be systematically built up and curated in a dedicated and not to be underestimated effort along the development. Rigorous configuration control is required for test data sets (including the CCDB), making them fully traceable. Test data set limitations should be documented at every development step. Test data should contain (i) synthetic, simple test data sets allowing simple verification along the development process, (ii) data sets using actual instrument data (in particular for internal calibration modes), (iii) state-of-the art scientific data sets, (iv) long data sets for GS verification.

705 Master repositories should be used for code, test data and documentation. The same item should not be stored in multiple places (other than synchronised repositories for backup).

Level 2 processor developers should be involved early in the L1 algorithm/product verification, with bread-boarding of critical modules. Development contracts should be short (not longer than 2.5 years) to keep flexibility. Agile developments are to be preferred, they worked very well for EarthCARE. All delivered code needs to be used immediately, regularly, and by as many people as possible, so issues can be identified and fixed early, while software developers are still familiar with the code.

710 We found that it worked well to have a set of general requirements and conventions across all processors and to limit allowed programming languages to the absolute minimum (C/C++/Fortran); this simplified the maintenance. Strict processor runtime requirements turned out to be very useful, forcing developers to optimise runtime. We had an efficient set-up of software support to the scientific level 2 processor developers, and the collaborative environment described in the previous section helped to coordinate the development in an efficient way.

7 Product format and conventions

7.1 Product format

EarthCARE level 1 and level 2 data products will be provided as NetCDF-4/HDF5 files. This format has been selected as it is widely used in the community and is self-describing. Furthermore, a large number of software tools and libraries are available to read this format. Products use internal data compression and each product covers one frame (1/8 orbit or about 5000 km along track).

7.2 Product conventions

For ESA products and processors, each data product name and each processor name consists of two parts, up to four letters XXXX, indicating the data origin and up to three letters YYY indicating data content, connected by a hyphen: XXX-YYY. For most products, XXX refers to one or more of the four EarthCARE instrument (A for ATLID, C for CPR, M for MSI, B for BBR). For example, the level 2a product A-FM refers to the feature mask (FM) derived from ATLID (A). Auxiliary data products X-MET and X-JSG (4) do not use any instrument measurements, so they use X instead of an instrument identifier.

JAXA data products are referenced by their product identifiers that are composed of two parts separated by an underscore (e.g. CPR_CLP). The first three letters indicate the instruments used in the product (CPR=CPR, ATL=ATLID, MSI=MSI,



730 AC=ATLID-CPR, ACM=ATLID-CPR-MSI, AM=ATLID-MSI, ALL=Four sensors) and the latter three letters indicates the geophysical content of the product (e.g. CLP for cloud properties and RAD for radiation).

Parameters and dimensions within the data products follow a common set of conventions, which aim to harmonise naming across products and to make the names as self-explanatory as possible. This means they can be rather long, as acronyms (apart from the instrument names) are avoided. Other conventions concern the use of units and of certain standard suffices, such as

735 “flag” for a parameter that can only assume the values 0 and 1.

8 Conclusions

We have presented an overview of the EarthCARE processors development, encompassing processors developed by teams in Europe, Japan and Canada. These will facilitate exploitation of the four instruments embarked on the EarthCARE satellite, which will fly in a sun-synchronous, low Earth orbit with a Mean Local Solar Time of 14:00 ±5 minutes. As well as the

740 single instrument products available at level 1 and level 2, a comprehensive set of multiple-instrument, synergistic, level 2 data products will retrieve aerosol, cloud, precipitation and radiation parameters. A Joint Standard Grid is generated and used to ensure that radar, lidar and multispectral image data is collocated such that the same column of the atmosphere is viewed. An auxiliary product contains a sub-set of meteorological fields from an ECMWF atmospheric model that covers the EarthCARE swath.

745 Test of the processing chain has made use of a dedicated End-to-End Simulator, called E3SIM, and special test data sets that were generated from data assimilated from multiple sources. E3SIM incorporates forward models and instrument simulators to generate the signals expected in Instrument Source Packets. The ISPs are ingested into the processor chain and outputs can be compared against the input data. A description of the collaborative development used in the processing chain development is presented as well as the lessons learnt.

750 All EarthCARE data products will be available from both ESA and JAXA website. An overview is given of EarthCARE product format and conventions, as well as a short summary of the different products’ contents and references to the dedicated papers that describe their algorithm and content in more detail.

EarthCARE will allow scientists to evaluate the representation of cloud, aerosol, precipitation and radiative flux in weather forecast and climate models, with the objective to improve parameterisation and, in particular, address uncertainty in cloud

755 processes.

Code and data availability. This overview paper refers generally to software code for level 2 processors and for atmospheric models that have been used to prepare data and simulations. The references for software repositories can be found in each of the dedicated papers that are contained within this special issue on EarthCARE level 2 algorithms and data products. The EarthCARE level 2 demonstration products from simulated scenes are available at <https://doi.org/10.5281/zenodo.7117115> (van Zadelhoff et al., 2023b).



760 *Author contributions.* ME prepared the manuscript and overview of the processing chain and level 2 processors, simulation and test. FM described the ATLID and BBR instrument and L1 processors. KW introduced the mission and described the MSI instrument and L1 processor, and the auxiliary processors. TK described the CPR instrument and L1 processor, with contributions from NT and YO. TT described the JAXA L2 processing chain. TW contributed to the science background and data product overview. DB, the ESA EarthCARE Project Manager, and ET, the JAXA Project Manager, provided overall guidance on the technical and programmatic context.

765 *Competing interests.* The authors declare that they have no conflict of interest.

Disclaimer. Publisher's note: Copernicus Publications remains neutral with regard to jurisdictional claims in published maps and institutional affiliations. Special issue statement. This article is part of the special issue "EarthCARE level 2 algorithms and data products". It is not associated with a conference.

Acknowledgements. We would like to recognise the industrial partners working on the satellite, payload and level 1 processors, led by
770 the satellite prime, Airbus Defence and Space (Germany), with instrument teams at NEC (Japan), SSTL (UK), Airbus Defence and Space (France), Thales Alenia Space (UK), and level 1 processors development and auxiliary processors development supported by GMV (UK) and S[&]T (NO) respectively. We thank the teams of scientists at several institutions in Europe, Japan and Canada that have developed EarthCARE level 2 processors and products, as well as at the ECMWF. Special thanks to members of the Joint Mission Advisory Group, which advises ESA and JAXA on science aspects of the mission, as well as to the principal investigators and project scientists of NASA
775 missions CloudSat and CALIPSO and the CERES instrument for their long-standing support and advice. We would also like to thank colleagues at ESA, JAXA and NICT, and particularly remember Tobias Wehr, EarthCARE Mission Scientist, who passed away suddenly and unexpectedly in 2023, after more than a decade of support to the mission.



References

- Barker, H. W., Cole, J. N. S., Qu, Z., Villefranque, N., and Shephard, M.: Radiative closure assessment of retrieved cloud and aerosol properties for the EarthCARE mission: the ACMB-DF product, *Atmospheric Measurement Techniques*, to be submitted, 2023.
- Cole, J. N. S., Barker, H. W., Qu, Z., Villefranque, N., and Shephard, M. W.: Broadband Radiative Quantities for the EarthCARE Mission: The ACM-COM and ACM-RT Products, *Atmospheric Measurement Techniques Discussions*, 2022, 1–37, <https://doi.org/10.5194/amt-2022-304>, 2022.
- Docter, N., Preusker, R., Filipitsch, F., Kritten, L., Schmidt, F., and Fischer, J.: Aerosol optical depth retrieval from the EarthCARE Multi-Spectral Imager: the M-AOT product, *Atmospheric Measurement Techniques*, 16, 3437–3457, <https://doi.org/10.5194/amt-16-3437-2023>, 2023.
- Donovan, D. P., Kollias, P., Velázquez Blázquez, A., and van Zadelhoff, G.-J.: The Generation of EarthCARE L1 Test Data sets Using Atmospheric Model Data Sets, *EGUsphere*, 2023, 1–54, <https://doi.org/10.5194/egusphere-2023-384>, 2023a.
- Donovan, D. P., van Zadelhoff, G.-J., and Wang, P.: The EarthCARE lidar cloud and aerosol profile processor: the A-AER, A-EBD, A-TC and A-ICE products, *Atmospheric Measurement Techniques*, to be submitted, 2023b.
- Feofilov, A. G., Chepfer, H., Noël, V., and Szczap, F.: Incorporating EarthCARE observations into a multi-lidar cloud climate record: the ATLID (Atmospheric Lidar) cloud climate product, *Atmospheric Measurement Techniques*, 16, 3363–3390, <https://doi.org/10.5194/amt-16-3363-2023>, 2023.
- Haarig, M., Hünerbein, A., Wandinger, U., Docter, N., Bley, S., Donovan, D., and van Zadelhoff, G.-J.: Cloud top heights and aerosol columnar properties from combined EarthCARE lidar and imager observations: the AM-CTH and AM-ACD products, *EGUsphere*, 2023, 1–32, <https://doi.org/10.5194/egusphere-2023-327>, 2023.
- Hagihara, Y.: Global assessments of Doppler velocity errors of EarthCARE CPR using NICAM, *Atmospheric Measurement Techniques*, to be submitted, 2023.
- Hagihara, Y., Okamoto, H., and Yoshida, R.: Development of a combined CloudSat-CALIPSO cloud mask to show global cloud distribution, *J. Geophys. Res.*, 115, 2010.
- Hagihara, Y., Ohno, Y., Horie, H., Roh, W., Satoh, M., Kubota, T., and Oki, R.: Assessments of Doppler Velocity Errors of EarthCARE Cloud Profiling Radar Using Global Cloud System Resolving Simulations: Effects of Doppler Broadening and Folding, *IEEE Trans. Geosci. Remote Sens.*, 60, 1–9, 2021.
- Hagihara, Y., Ohno, Y., Horie, H., Roh, W., Satoh, M., and Kubota, T.: Global evaluation of Doppler velocity errors of Earth-CARE cloud-profiling radar using a global storm-resolving simulation, *Atmospheric Measurement Techniques*, 16, 3211–3219, <https://doi.org/10.5194/amt-16-3211-2023>, 2023.
- Hünerbein, A., Bley, S., Deneke, H., Meirink, J. F., van Zadelhoff, G.-J., and Walther, A.: Cloud optical and physical properties retrieval from EarthCARE multi-spectral imager: the M-COP products, *EGUsphere*, 2023, 1–23, <https://doi.org/10.5194/egusphere-2023-305>, 2023a.
- Hünerbein, A., Bley, S., Horn, S., Deneke, H., and Walther, A.: Cloud mask algorithm from the EarthCARE Multi-Spectral Imager: the M-CM products, *Atmospheric Measurement Techniques*, 16, 2821–2836, <https://doi.org/10.5194/amt-16-2821-2023>, 2023b.
- IPCC: Climate Change 2021 – The Physical Science Basis: Working Group I Contribution to the Sixth Assessment Report of the Intergovernmental Panel on Climate Change, Masson-Delmotte, V., P. Zhai, A. Pirani, S.L. Connors, C. Péan, S. Berger, N. Caud, Y. Chen, L. Goldfarb, M.I. Gomis, M. Huang, K. Leitzell, E. Lonnoy, J.B.R. Matthews, T.K. Maycock, T. Waterfield, O. Yelekçi, R. Yu, and B.



- 815 Zhou (eds.), Cambridge University Press, Cambridge, United Kingdom and New York, NY, USA, <https://doi.org/10.1017/9781009157896>, 2023.
- Irbah, A., Delanoë, J., van Zadelhoff, G.-J., Donovan, D. P., Kollias, P., Puigdomènech Treserras, B., Mason, S., Hogan, R. J., and Tatarevic, A.: The classification of atmospheric hydrometeors and aerosols from the EarthCARE radar and lidar: the A-TC, C-TC and AC-TC products, *Atmospheric Measurement Techniques*, 16, 2795–2820, <https://doi.org/10.5194/amt-16-2795-2023>, 2023.
- 820 Kikuchi, M., Okamoto, H., Sato, K., Suzuki, K., Cesana, G., Hagihara, Y., Takahashi, N., Hayasaka, T., and Oki, R.: Development of algorithm for discriminating hydrometeor particle types with a synergistic Use of CloudSat and CALIPSO, *Journal of Geophysical Research: Atmospheres*, 122, 11–022, 2017.
- Kollias, P., Puidgomènech Treserras, B., Battaglia, A., Borque, P. C., and Tatarevic, A.: Processing reflectivity and Doppler velocity from EarthCARE's cloud-profiling radar: the C-FMR, C-CD and C-APC products, *Atmospheric Measurement Techniques*, 16, 1901–1914, <https://doi.org/10.5194/amt-16-1901-2023>, 2023.
- 825 Kudo, R., Nishizawa, T., and Aoyagi, T.: Vertical profiles of aerosol optical properties and the solar heating rate estimated by combining sky radiometer and lidar measurements, *Atmospheric Measurement Techniques*, 9, 3223–3243, 2016.
- Letu, H., Ishimoto, H., Riedi, J., Nakajima, T. Y., C-Labonnote, L., Baran, A. J., Nagao, T. M., and Sekiguchi, M.: Investigation of ice particle habits to be used for ice cloud remote sensing for the GCOM-C satellite mission, *Atmospheric Chemistry and Physics*, 16, 12 287–12 303, 2016.
- 830 Letu, H., Nagao, T. M., Nakajima, T. Y., Riedi, J., Ishimoto, H., Baran, A. J., Shang, H., Sekiguchi, M., and Kikuchi, M.: Ice cloud properties from Himawari-8/AHI next-generation geostationary satellite: Capability of the AHI to monitor the DC cloud generation process, *IEEE Transactions on Geoscience and Remote Sensing*, 57, 3229–3239, 2018.
- Mason, S. L., Cole, J. N. S., Docter, N., Donovan, D. P., Hogan, R. J., Hünerbein, A., Kollias, P., Puigdomènech Treserras, B., Qu, Z., Wandinger, U., and van Zadelhoff, G.-J.: An intercomparison of EarthCARE cloud, aerosol and precipitation retrieval products, *EGU-sphere*, 2023, 1–34, <https://doi.org/10.5194/egusphere-2023-1682>, 2023a.
- 835 Mason, S. L., Hogan, R. J., Bozzo, A., and Pounder, N. L.: A unified synergistic retrieval of clouds, aerosols, and precipitation from EarthCARE: the ACM-CAP product, *Atmospheric Measurement Techniques*, 16, 3459–3486, <https://doi.org/10.5194/amt-16-3459-2023>, 2023b.
- Mroz, K., Treserras, B. P., Battaglia, A., Kollias, P., Tatarevic, A., and Tridon, F.: Cloud and precipitation microphysical retrievals from the EarthCARE Cloud Profiling Radar: the C-CLD product, *Atmospheric Measurement Techniques*, 16, 2865–2888, <https://doi.org/10.5194/amt-16-2865-2023>, 2023.
- 840 Nakajima, T. Y., Ishida, H., Nagao, T. M., Hori, M., Letu, H., Higuchi, R., Tamaru, N., Imoto, N., and Yamazaki, A.: Theoretical basis of the algorithms and early phase results of the GCOM-C (Shikisai) SGLI cloud products, *Progress in Earth and Planetary Science*, 6, 1–25, 2019.
- 845 Nishizawa, T.: Algorithms to retrieve aerosol optical properties from ATLID/EarthCARE and CALIOP/CALIPSO, *Atmospheric Measurement Techniques*, to be submitted, 2023.
- Nishizawa, T., Sugimoto, N., Matsui, I., Shimizu, A., Tatarov, B., and Okamoto, H.: Algorithm to retrieve aerosol optical properties from high-spectral-resolution lidar and polarization Mie-scattering lidar measurements, *IEEE Transactions on Geoscience and Remote Sensing*, 46, 4094–4103, 2008.



- 850 Nishizawa, T., Sugimoto, N., Matsui, I., Shimizu, A., and Okamoto, H.: Algorithms to retrieve optical properties of three component aerosols from two-wavelength backscatter and one-wavelength polarization lidar measurements considering nonsphericity of dust, *Journal of Quantitative Spectroscopy and Radiative Transfer*, 112, 254–267, 2011.
- Nishizawa, T., Kudo, R., Higure, A., Oikawa, E., and Hajime, O.: Aerosol and Cloud Retrieval Algorithms Using EarthCARE Satellite-borne Lidar Data (in Japanese), *Journal of the Remote Sensing Society of Japan*, 39, 215–224,
855 <https://doi.org/https://doi.org/10.11440/rssj.39.215>, 2019.
- Oikawa, E.: Improvement of cloud mask algorithm for EarthCARE ATLID (tentative), *Atmospheric Measurement Techniques*, to be submitted, 2023.
- Oikawa, E., Nakajima, T., Inoue, T., and Winker, D.: A study of the shortwave direct aerosol forcing using ESSP/CALIPSO observation and GCM simulation, *Journal of Geophysical Research: Atmospheres*, 118, 3687–3708, 2013.
- 860 Oikawa, E., Nakajima, T., and Winker, D.: An evaluation of the shortwave direct aerosol radiative forcing using CALIOP and MODIS observations, *Journal of Geophysical Research: Atmospheres*, 123, 1211–1233, 2018.
- Okamoto, H.: New perspectives of clouds, radiation and dynamics from EarthCARE observation (tentative), *Atmospheric Measurement Techniques*, to be submitted, 2023.
- Okamoto, H., Nishizawa, T., Takemura, T., Kumagai, H., Kuroiwa, H., Sugimoto, N., Matsui, I., Shimizu, A., Emori, S., Kamei, A., et al.:
865 Vertical cloud structure observed from shipborne radar and lidar: Midlatitude case study during the MR01/K02 cruise of the research vessel Mirai, *Journal of Geophysical Research: Atmospheres*, 112, 2007.
- Okamoto, H., Nishizawa, T., Takemura, T., Sato, K., Kumagai, H., Ohno, Y., Sugimoto, N., Shimizu, A., Matsui, I., and Nakajima, T.: Vertical cloud properties in the tropical western Pacific Ocean: Validation of the CCSR/NIES/FRCGC GCM by shipborne radar and lidar, *Journal of Geophysical Research: Atmospheres*, 113, 2008.
- 870 Okamoto, H., Sato, K., and Hagihara, Y.: Global analysis of ice microphysics from CloudSat and CALIPSO: Incorporation of specular reflection in lidar signals, *Journal of Geophysical Research: Atmospheres*, 115, 2010.
- Okata, M., Nakajima, T., Suzuki, K., Inoue, T., Nakajima, T., and Okamoto, H.: A study on radiative transfer effects in 3-D cloudy atmosphere using satellite data, *Journal of Geophysical Research: Atmospheres*, 122, 443–468, 2017.
- Qu, Z., Donovan, D. P., Barker, H. W., Cole, J. N. S., Shephard, M. W., and Huijnen, V.: Numerical Model Generation of Test Frames for Pre-
875 launch Studies of EarthCARE’s Retrieval Algorithms and Data Management System, *Atmospheric Measurement Techniques Discussions*, 2022, 1–31, <https://doi.org/10.5194/amt-2022-300>, 2022.
- Qu, Z., Barker, H. W., Cole, J. N. S., and Shephard, M. W.: Across-track extension of retrieved cloud and aerosol properties for the EarthCARE mission: the ACMB-3D product, *Atmospheric Measurement Techniques*, 16, 2319–2331, <https://doi.org/10.5194/amt-16-2319-2023>, 2023.
- 880 Roh, W., Satoh, M., Hashino, T., Matsugishi, S., Nasuno, T., and Kubota, T.: Introduction to EarthCARE synthetic data using a global storm-resolving simulation, *Atmospheric Measurement Techniques*, 16, 3331–3344, <https://doi.org/10.5194/amt-16-3331-2023>, 2023.
- Sato, K.: EarthCARE cloud-precipitation and air-motion products (tentative), *Atmospheric Measurement Techniques*, to be submitted, 2023.
- Sato, K. and Okamoto, H.: Refinement of global ice microphysics using spaceborne active sensors, *Journal of Geophysical Research: Atmospheres*, 116, 2011.
- 885 Sato, K., Okamoto, H., Yamamoto, M. K., Fukao, S., Kumagai, H., Ohno, Y., Horie, H., and Abo, M.: 95-GHz Doppler radar and lidar synergy for simultaneous ice microphysics and in-cloud vertical air motion retrieval, *Journal of Geophysical Research: Atmospheres*, 114, 2009.



- van Zadelhoff, G.-J., Donovan, D. P., and Wang, P.: Detection of aerosol and cloud features for the EarthCARE atmospheric lidar (ATLID): the ATLID Feature Mask (A-FM) product, *Atmospheric Measurement Techniques*, 16, 3631–3651, <https://doi.org/10.5194/amt-16-3631-2023>, 2023.
- 890
- Velázquez Blázquez, A., Baudrez, E., Clerbaux, N., and Domenech, C.: Unfiltering of the EarthCARE Broadband Radiometer (BBR) observations: the BM-RAD product, *Atmospheric Measurement Techniques Discussions*, 2023, 1–16, <https://doi.org/10.5194/amt-2023-170>, 2023a.
- Velázquez Blázquez, A., Baudrez, E., Clerbaux, N., Domenech, C., Marañón, R. G., and Madenach, N.: Retrieval of top-of-atmosphere fluxes from combined EarthCARE lidar, imager and broadband radiometer observations: the BMA-FLX product, *Atmospheric Measurement Techniques*, to be submitted, 2023b.
- 895
- Wandinger, U., Haarig, M., Baars, H., Donovan, D., and van Zadelhoff, G.-J.: Cloud top heights and aerosol layer properties from EarthCARE lidar observations: the A-CTH and A-ALD products, *EGUsphere*, 2023, 1–32, <https://doi.org/10.5194/egusphere-2023-748>, 2023.
- Wang, M., Nakajima, T. Y., Roh, W., Satoh, M., Suzuki, K., Kubota, T., and Yoshida, M.: Evaluation of the spectral misalignment on the Earth Clouds, Aerosols and Radiation Explorer/multi-spectral imager cloud product, *Atmospheric Measurement Techniques*, 16, 603–623, <https://doi.org/10.5194/amt-16-603-2023>, 2023.
- 900
- Wehr, T., Kubota, T., Tzeremes, G., Wallace, K., Nakatsuka, H., Ohno, Y., Koopman, R., Rusli, S., Kikuchi, M., Eisinger, M., Tanaka, T., Taga, M., Deghaye, P., Tomita, E., and Bernaerts, D.: The EarthCARE mission – science and system overview, *Atmospheric Measurement Techniques*, 16, 3581–3608, <https://doi.org/10.5194/amt-16-3581-2023>, 2023.
- 905
- Yamauchi, A.: Description and validation of Japanese standard algorithm for radiative flux and heating rate products with EarthCARE 4 sensors, *Atmospheric Measurement Techniques*, to be submitted, 2023.
- Yoshida, M., Kikuchi, M., Nagao, T. M., Murakami, H., Nomaki, T., and Higurashi, A.: Common retrieval of aerosol properties for imaging satellite sensors, *Journal of the Meteorological Society of Japan. Ser. II*, 2018.
- Yoshida, R., Okamoto, H., Hagihara, Y., and Ishimoto, H.: Global analysis of cloud phase and ice crystal orientation from Cloud-Aerosol Lidar and Infrared Pathfinder Satellite Observation (CALIPSO) data using attenuated backscattering and depolarization ratio, *Journal of Geophysical Research: Atmospheres*, 115, 2010.
- 910